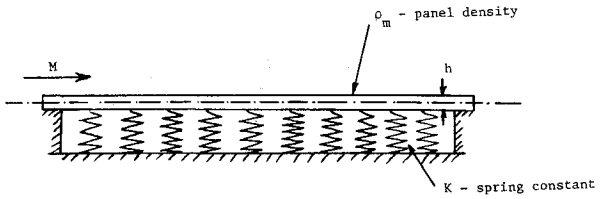

Fig. 1 A finite panel resting on elastic springs.

effect of aerodynamic damping on panel flutter at supersonic Mach numbers for various configurations, has also discussed the problem of a panel resting on an elastic foundation.

In this paper, the flutter behavior of a thin panel resting on a linear elastic foundation is studied, using an analogy with the flutter of a panel of the same geometry without spring support.

Analysis

Consider a flat panel of finite dimensions exposed to supersonic flow on its upper surface and to still air on the other side (Fig. 1). The panel rests on an elastic foundation, which is mathematically idealized as closely spaced linear springs. Using quasi-steady theory for the aerodynamic loading, Dugundji[6] has made an exact linear analysis of the equations representing flutter of such configurations. The critical flutter condition occurs when the total damping of the system becomes zero, and the results can be seen from Eqs. (26) and (27) of Ref. 6,

$$Q_I/(-Q_R)^{1/2} = g_T \tag{1}$$

and

$$(-Q_R)^{1/2} = \omega_{F_e} \tag{2}$$

All the above parameters are defined in Ref. 6. Here Q_R and Q_I refer to the composite system and $\bar{Q}_R$ and $\bar{Q}_I$ represent the system without the springs; it can be seen that $\bar{Q}_R = Q_R + k$ and $\bar{Q}_I = Q_I$. Placing these parameters into the above equations and rearranging, one may obtain

$$g_{T_e} = g_T(1+\gamma)^{1/2} \tag{3}$$

$$\omega_{F_e} = \omega_F(1+\gamma)^{1/2} \tag{4}$$

where

$$\gamma = (K/\rho_m h)/\omega_F{}^2$$

Here, ω_{F_e} is the flutter frequency of the panel supported on elastic foundation, and ω_F is the flutter frequency of the same panel without elastic support. Eq. (3) can be interpreted as a modification of the effective damping of the panel due to the presence of the elastic foundation. Because of the increase in total damping, the flutter velocity of the panel generally increases with the stiffness of the springs (see Fig. 5 of Ref. 6).

In Ref. 6, it was found that for low values of the damping coefficient g_T, the flutter dynamic pressure parameter λ_F is independent of g_T; for high values of g_T, λ_F is roughly proportional to it. A similar interpretation may also be given for g_{T_e}. This means that for a low value of g_T, λ_F increases directly with g_{T_e}. This also suggests that for low values of g_{T_e}, it is possible to use the quasi-static (Ackeret) approximation for aerodynamic loading with reasonable accuracy. Further, it can also be found from Ref. 6 that flutter modes change from standing waves at low values of g_{T_e} to traveling waves at high values of g_{T_e}. Hence, the presence of springs not only affects the flutter velocity and the flutter frequency of the panel, but can also change the type of flutter mode, depending upon the support stiffness.

Some comment may be made concerning the flutter of two parallel panels joined by an elastic medium, a problem discussed in Refs. 4 and 5. Here, because of the coupling of the motion of the two plates in the presence of elastic springs, the dynamic characteristics of this composite system are quite different from those of individual panels. Depending upon the inplane forces, the flutter characteristics of this configuration are very much affected by the stiffness of the elastic medium, regardless of whether or not damping is considered.

Conclusion

Using a simple analogy, the flutter characteristics of a uniform panel resting on a linear elastic foundation can be easily obtained from those of a panel of the same geometry with no elastic support. Using quasi-steady aerodynamic loading, it may be observed that there is not only a change in the flutter frequency, but also of the total damping of the system, due to the elastic foundation. Further, it is found that for small values of aerodynamic damping and spring stiffness, the quasi-static approach is reasonable, whereas for high values of aerodynamic damping or of spring stiffness, quasi-static theory will not be adequate. Also, for high values of spring stiffness the flutter mode of the panel exhibits traveling wave motion.

References

[1] Dugundji, J., Dowell, E., and Perkin, B., "Subsonic Flutter of Panels on Continuous Elastic Foundations," *AIAA Journal*, Vol. 1, May 1963, pp. 1146–1154.

[2] Miles, J. W., "On the Aerodynamic Instability of Thin Panels," *Journal of the Aeronautical Sciences*, Vol. 23, Aug. 1956, pp. 771–791.

[3] Johns, D. J., "Static Instability of Rectangular Orthotropic Panels Subjected to Uniform In-plane Loads and Deflection Dependent Lateral Loads," R. & M. 3569, Aeronautical Research Council, London, 1969.

[4] McElman, J. A., "Flutter of Two Parallel Flat Plates Connected by an Elastic Media," *AIAA Journal*, Vol. 2, Feb. 1964, pp. 377–379.

[5] Johns, D. J. and Taylor, P. W., "Vibration and Flutter of Parallel Flat Plates Connected by an Elastic Media," AIAA/ASME 11th Structures, Structural Dynamics and Materials Conference, Denver, Colo. April 1970.

[6] Dugundji, J., "Theoretical Considerations of Panel Flutter at High Supersonic Mach Numbers," *AIAA Journal*, Vol. 4, July 1966, pp. 1257–1266.

Laminar Separated Flow over Nonlifting Ellipses

NATHAN NESS*
West Virginia University, Morgantown, West Va.

FIGURES 1 and 2 present the results of calculations for the laminar separated flow over nonlifting ellipses as functions of the thickness/chord ratio t/c and the freestream Reynolds number Re_∞ ($= V_\infty c/\nu$). The results include the laminar separated flow over the circular cylinder as the special case when $(t/c) = 1$. The calculations involve a coupling of inviscid and viscid flow, i.e., the inviscid analysis provides the pressure which is used in the boundary-layer program to locate the boundary-layer separation points.

The inviscid calculations are based on the work of Parkinson and Jandali[1] who determined the effect of the wake on several symmetrical nonlifting blunt bodies. Their theoretical model provides an expression for the pressure distribution along the wetted surface PLQ of the body (Fig. 1), an expression for the asymptotic wake height H, and an expression for the pressure

Received August 15, 1974; revision received September 19, 1974. This work was developed for the Office of Naval Research under Navy V/STOL Aerodynamics Contract N00014-68-A-0512. The author acknowledges E. H. Gibbs, Instructor; Y.-T. T. Lin, Graduate Research Assistant; and H.-F. Wang, Graduate Research Assistant; all from the Department of Aerospace Engineering, West Virginia University, for programing and performing the present calculations.

Index category: Jets, Wakes, and Viscid-Inviscid Flow Interactions.

* Professor of Aerospace Engineering. Associate Fellow AIAA.

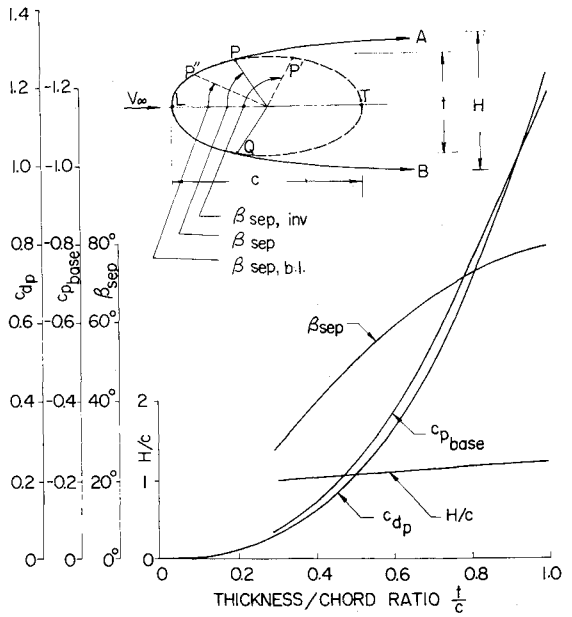

Fig. 1 H/c, β_{sep}, $c_{p_{base}}$, c_{d_p} **as functions of the thickness/chord ratio. (Note: These results are for laminar separation only and are independent of** Re_∞**).**

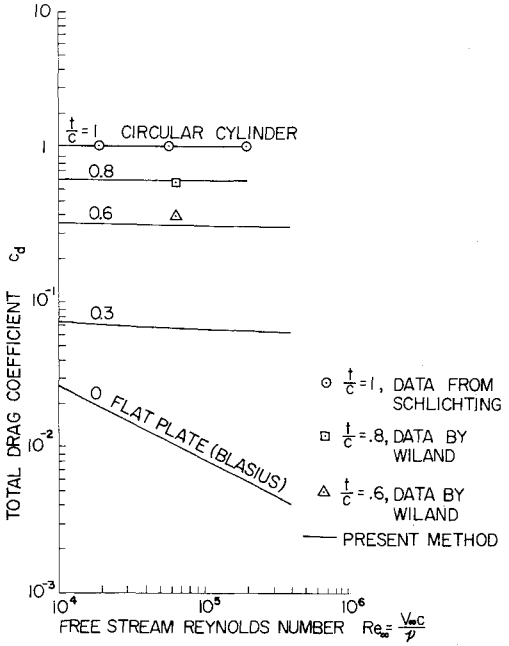

Fig. 2 Total drag coefficient vs freestream Reynolds number.

distribution along the separation streamlines PA, QB which decreases asymptotically to the freestream pressure at infinity downstream. The theory in Ref. 1 is inviscid only and requires an experimental value for the base pressure (assumed constant over the base region PTQ) to locate the separation points P, Q.

Bluston and Paulson[2] applied the theory of Ref. 1 to the laminar separated flow over a circular cylinder. They introduced the boundary-layer equations into the analysis thereby enabling them to determine the separation points P, Q analytically. The analysis in Ref. 2 involves iteration and proceeds as follows. A separation angle $\beta_{sep,inv}$ is assumed (Fig. 1) and the Parkinson et al. method[1] is used to provide the pressure distribution over the wetted portion LP'. A boundary-layer analysis is then employed starting at the forward stagnation point L and proceeding downstream along the cylinder until boundary-layer separation is attained at point P''. This provides the angle $\beta_{sep,b.l.}$ corresponding to the arc LP''. This angle is compared to the assumed inviscid separation angle $\beta_{sep,inv}$. The procedure is repeated until the difference in the angles $\beta_{sep,inv} - \beta_{sep,b.l.}$ is less than some prescribed small value. At this condition the solution is unique.

The present analysis differs from that in Ref. 2 in the following ways. 1) The present analysis applies to ellipses whereas Ref. 2 considered only the circular cylinder. 2) The present analysis uses the finite difference method of Ref. 3 for the solution of the boundary layer equations. 3) The present analysis uses a search method to indicate convergence between the assumed inviscid separation angle $\beta_{sep,inv}$ and the boundary-layer separation angle $\beta_{sep,b.l.}$. The search method involves assuming values for $\beta_{sep,inv}$ until (within the accuracy of the calculations) its value and that of $\beta_{sep,b.l.}$ are equal. The solution is then unique and provides the dimensionless asymptotic wake height H/c, the streamline separation angle β_{sep}, the pressure coefficient at the base of the body $c_{p_{base}}$ (assumed constant over the region PTQ), the pressure coefficient and the skin friction coefficient on the wetted portion PLQ. Integration of the pressure coefficients provides the pressure drag coefficient c_{d_p} and integration of the skin friction coefficient provides the skin friction drag coefficient c_{d_f}. Their sum gives the total sectional drag coefficient c_d.

Calculations were performed for $(t/c) = 0$, 0.3, 0.6, 0.8, 1 and for freestream Reynolds numbers Re_∞ from 10^4 to 4×10^5. Results are presented only for those combinations of t/c and Re_∞ which resulted in laminar separation.

Figure 1 shows the dimensionless wake height H/c, the streamline separation angle β_{sep}, the base pressure coefficient $c_{p_{base}}$, and the pressure drag coefficient c_{d_p} as functions of t/c. For laminar separation the calculations show that these results are independent of Re_∞. The dimensionless wake height remains practically constant for the range of t/c considered: it decreases from $(H/c) = 1.23$ at $(t/c) = 1$ to $(H/c) = 1.02$ at $(t/c) = 0.3$. The streamline separation angle decreases from $\beta_{sep} = 80°$ at $(t/c) = 1$ to $\beta_{sep} = 28°$ at $(t/c) = 0.3$. The decrease in β_{sep} as t/c decreases is probably due to the increased adverse pressure gradient as the nose radius decreases. The base pressure coefficient has the value $c_{p_{base}} = -1.18$ at $(t/c) = 1$ and appears to be approaching zero as t/c goes to zero. The pressure drag coefficient has the value $c_{d_p} = 1.24$ at $(t/c) = 1$ and decreases to zero for the flat plate, $(t/c) = 0$. Some test data from the literature are as follows: Hiemenz (p. 162, Ref. 4) for laminar separation over a circular cylinder obtained $\beta_{sep} = 81°$. The value of Re_∞ is not given. Roshko[5] from tests on a circular cylinder for laminar separation at $Re_\infty = 1.45 \times 10^4$ obtained $\beta_{sep} = 80°$, $c_{p_{base}} = -0.96$. Wiland[6] from tests on ellipses for laminar separation at $Re_\infty = 6.8 \times 10^4$ obtained for the base pressure coefficient the following: $(t/c) = 0.8$, $c_{p_{base}} = -0.96$; $(t/c) = 0.6$, $c_{p_{base}} = -0.71$. It is noted that Wiland obtained the same value for the base pressure coefficient at $(t/c) = 0.8$ as Roshko did for the circular cylinder. Correlation of the theoretical curve with test data for $c_{p_{base}}$ is poor; correlation of theory with test data for β_{sep} is good. The test points are not shown in Fig. 1 in order to keep that figure uncluttered.

Figure 2 presents the total drag coefficient c_d as a function of the freestream Reynolds number at constant values of t/c. The solid lines in the figure represent the theoretical curves and include the skin friction coefficient c_{d_f}. The skin friction contribution to the over-all drag increases as t/c and Re_∞ decrease. At $(t/c) = 1$ and $Re_\infty = 2 \times 10^5$ the skin friction drag is only 0.5% of the total drag; at $(t/c) = 0.3$ and $Re_\infty = 10^4$ the skin friction drag has increased to 17% of the total drag while for the flat plate, the total drag, of course, is all skin friction drag. These observations explain the slope of the curves in Fig. 2. At $(t/c) = 1$ the total drag is practically all pressure drag and as shown in Fig. 1 remains constant with Re_∞; hence for $(t/c) = 1$ the c_d vs Re_∞ curve is horizontal. As t/c decreases the skin friction drag, which depends on Re_∞, contributes a larger percentage to the over-all drag. The result is that the slope of the c_d vs Re_∞ curve becomes more negative and approaches the flat plate slope in the limit as t/c approaches zero. The flat plate result in Fig. 2 is obtained from the Blasius relation [Eq. (7.34), Ref. 4]. Included in the figure are several test points. Those for the circular cylinder

were obtained from Fig. 1.4, Ref. 4, while those for the ellipses were obtained by Wiland[6] at $Re_\infty = 6.8 \times 10^4$. Wiland's results, after being corrected as indicated on page 60 of his report are: $(t/c) = 0.8$, $c_d = 0.67$; $(t/c) = 0.6$, $c_d = 0.40$. These test results are compared to the theoretical values: $(t/c) = 0.8$, $c_d = 0.71$; $(t/c) = 0.6$, $c_d = 0.34$. Thus the percentage deviation of the theoretical value from the experimental value is as follows. For $(t/c) = 0.8$, percentage deviation = 6%; for $(t/c) = 0.6$, percentage deviation = 15%. Details of the analysis, the computer program, and additional results are contained in Ref. 7.

In conclusion, the method presented here for the laminar separated flow over nonlifting ellipses appears to be in reasonable agreement with the available experimental data especially for the drag coefficient.

References

[1] Parkinson, G. V. and Jandali, T., "A Wake Source Model for Bluff Body Potential Flow," *Journal of Fluid Mechanics*, Vol. 40, Pt. 3, 1970, pp. 577–594.

[2] Bluston, H. S. and Paulson, R. W., "A Theoretical Solution for Laminar Flows Past a Bluff Body with a Separated Wake," *Journal de Mécanique*, Vol. 11, March 1972, pp. 161–180.

[3] Cebeci, T., Smith, A. M. O., and Wang, L. C., "A Finite-Difference Method for Calculating Compressible Laminar and Turbulent Boundary Layers," Rept. DAC-67131, March 1969, Douglas Aircraft Company, St. Louis, Mo.

[4] Schlichting, H., *Boundary-Layer Theory*, 6th ed., McGraw-Hill, New York, 1968.

[5] Roshko, A., "A New Hodograph for Free Streamline Theory," TN 3168, July 1954, NACA.

[6] Wiland, E., "Unsteady Aerodynamics of Stationary Elliptic Cylinders in Subcritical Flow," M.S. thesis, Department of Mechanical Engineering, The University of British Columbia, Vancouver, B.C., Canada, April 1968.

[7] Ness, N., Lin, Y.-T. T., and Wang, H.-F., "Laminar Separated Flow over Nonlifting Ellipses," TR-41, Department of Aerospace Engineering, West Virginia University, Morgantown, West Va., 1974.

Galerkin Finite Element Solution for the Stability of Cantilever Columns Subjected to Tangential Loads

G. VENKATESWARA RAO* AND R. V. NARASIMHA RAO*

Space Science and Technology Centre, Trivandrum, India

Introduction

STABILITY of nonconservative systems has been well discussed in the works of Bolotin[1] and Leipholz.[2] Recently, the finite element method has been successfully applied to the stability analysis of nonconservative systems. Barsoum[3] developed a finite element formulation based on the variational approach, whereas Kikuchi[4] presented a finite element formulation based on Mikhlin's[5] work on the Galerkin method. It is interesting to note that both the above formulations[3,4] gave identical element matrices for the stability analysis of cantilever column with a concentrated tangential load at the free end. In this Note, a different finite element formulation based on the weighted residual method using the Galerkin criterion is presented. Three problems concerning the stability of uniform cantilever column subjected to tangential loads are presented. The results indicate that the convergence of the present finite element method is excellent and even with a two-element idealization, very accurate results are obtained.

Received September 5, 1974. The authors take this opportunity to thank C. L. Amba-Rao for his constant encouragement throughout the course of this work.

Index category: Structural Stability Analysis.

* Engineer, Structural Engineering Division.

Finite Element Formulation

The differential equation governing the lateral motion of a column with tangential load, in the nondimensional form, is given by ($x = 0$ is fixed end and $x = 1$ is the free end).

$$W'''' + \lambda f(x) W'' - \Omega W = 0 \tag{1}$$

where $'$ denotes differentiation with respect to x. Here, three cases are considered:

Case 1: Subtangential concentrated load P at the free end for which $\lambda = PL^2/EI$ and $f(x) = 1$, where L is the length of the column, E is the Young's modulus and I is the moment of inertia.

Case 2: A uniformly distributed tangential load of intensity q_o per unit length, for which $\lambda = q_o L^3/EI$ and $f(x) = (1-x)$.

Case 3: A triangularly varying tangential load q of intensity $q = q_o(1-x)$, for which

$$\lambda = q_o L^4/EI \quad \text{and} \quad f(x) = \tfrac{1}{2}(1-x)^2$$

Ω is the frequency parameter defined as $\Omega = m\omega^2 L^4/EI$, where m is the mass of the column per unit length and ω is the circular frequency.

The boundary conditions are:

1) at $x = 0$ $\quad W = 0$ and $W' = 0$ (2)

2) at $x = 1$ $\quad W'' = 0$ and $W''' - \lambda(\gamma - 1)W' = 0$ (for case 1) (3)

(Here $\gamma = 0$ represents Euler column and $\gamma = 1$ represents Beck's[6] column) $W''' = 0$ (for cases 2 and 3).

In the present finite element formulation, the domain of the column is subdivided into a number of elements. A seventh degree polynomial in x is assumed over each element as

$$W_e = [1 \;\; x \;\; x^2 \;\; x^3 \;\; x^4 \;\; x^5 \;\; x^6 \;\; x^7]\{\alpha\}_e \tag{4}$$

where

$$\{\alpha\}_e{}^T = [\alpha_1 \;\; \alpha_2 \;\; \alpha_3 \;\; \alpha_4 \;\; \alpha_5 \;\; \alpha_6 \;\; \alpha_7 \;\; \alpha_8] \tag{5}$$

Equation (4) is concisely written as

$$W_e = [F]\{\alpha\}_e \tag{6}$$

The eight undetermined coefficients α_1–α_8 are determined by the nodal parameters W, W', W'', W''' at each end of the element as

$$\{\delta\}_e = [T]\{\alpha\}_e \tag{7}$$

where

$$\{\delta\}_e{}^T = [W_1 \;\; W_1' \;\; W_1'' \;\; W_1''' \;\; W_2 \;\; W_2' \;\; W_2'' \;\; W_2'''] \tag{8}$$

From Eqs. (6) and (7), we obtain

$$W_e = [\phi]\{\delta\}_e \tag{9}$$

where

$$[\phi] = [F][T]^{-1} \tag{10}$$

Substituting Eq. (9) in Eq. (1) we get the residual R_e for the element as

$$R_e = [\phi'']\{\delta\}_e + \lambda f(x)[\phi'']\{\delta\}_e - \Omega[\phi]\{\delta\}_e \tag{11}$$

In the Galerkin finite element method, the weighted residual is minimized as

$$\frac{\partial}{\partial\{\delta\}_e}\int W_e \cdot R_e \, dx = 0 \tag{12}$$

The process is repeated for all the elements and after the usual assembly procedure, one gets the matrix equation as

$$[K]\{\delta\} + \lambda[K_G]\{\delta\} - \Omega[M]\{\delta\} = 0 \tag{13}$$

where $\{\delta\}$ is the vector of nodal displacements of the structure.

The critical load λ_{cr} is obtained from Eq. (13) following the well known dynamic criterion where the two lowest frequencies just degenerate. It is to be noted here that the boundary conditions represented in Eqs. (2) and (3) can be easily satisfied for cases (2) and (3) in the present formulation. For case (1), a congruent transformation has to be effected so that $[W''' - \lambda(\gamma - 1)W']$ will